Roughness and Condition Prediction Models for Airfield Pavements using Digital Image Processing

First author:

Diego Cereceda
Graduate Student | Civil Engineering
Email : diego.cereceda@mail.udp.cl
Affiliation : School of Civil Engineering
Faculty of Engineering and Sciences
Universidad Diego Portales
Chile

Second author and corresponding author:

Carlos Medel-Vera, PhD
Assistant Professor | Civil Engineering
Email : cbmedel@uc.cl; carlos.medel@udp.cl
Affiliation : School of Civil Engineering
Faculty of Engineering and Sciences
Universidad Diego Portales
Chile

Third author:

Mauricio Ortiz
Civil Engineer | Project Engineer
Email : jose.ortiz.o@mop.gov.cl
Affiliation : Division of Airports
Ministry of Public Works
Chile

Fourth author:

José Tramon
Civil Engineer | Head of Construction Department
Email : jose.tramon@mop.gov.cl
Affiliation : Division of Airports
Ministry of Public Works
Chile

Roughness and Condition Prediction Models for Airfield Pavements using Digital Image Processing

Abstract

Based on the assessment of three runways at mid-size Chilean airports, the aim of this article is twofold. First, it discusses the potential empirical relationship that may exist between two parameters traditionally used to measure pavement roughness and condition, i.e. the International Roughness Index (IRI) and Pavement Condition Index (PCI), both measured using industry-standard, semi-automated processes. Second, it proposes an automated and parsimonious methodology for estimating the IRI and PCI, based on a digital image processing algorithm that accurately determines the total amount of cracking in pavements and which essentially requires no human curation. On one hand, a direct correlation between IRI and PCI has been obtained that can be considered statistically significant. On the other hand, highly reasonable estimates for the IRI and PCI can be achieved based solely on the total cracking percentage of a unit sample. The models proposed can be used for airport pavement management purposes.

Keywords

airport pavement management system; IRI vs. PCI model; automatic IRI estimation; automatic PCI estimation

1 Introduction

The management of airport pavements has over time become a progressively critical task due to ageing and deterioration, funding has become more restrictive, and potential disruption of operations must be highly minimised [1]. To appropriately manage airport pavements, several quality indices must be evaluated. These can be: (i) directly measured following a prescribed procedure (i.e. an objective approach), (ii) estimated by visual surveys based on judgement (i.e. a subjective approach), or (iii) determined by using a combination of both approaches [2]. The quality indices that are typically used for airport pavement management aim to assess physical properties such as load-bearing capacity, longitudinal and transverse

surface evenness, skid resistance, and pavement distress [3]. Two properties that are the subject of intensive research in airport pavement engineering are roughness and condition. Runways are subjected to increasingly heavy dynamic loads, as well as harsher weather conditions [4]. As such, their timely and effective assessment is critical for safe aircraft operations. Poor runway maintenance should be addressed from three perspectives, based on the potential negative results that may arise from these as follows: (i) a social perspective, as veer-off accidents can occur with potentially serious health effects for passengers and crew members [5, 6], (ii) an economic perspective, as costs can be adequately covered, e.g. those associated with cumulative damage to aircraft landing gear and airport disruption [7], and (iii) an environmental perspective, as there could be increased ecological costs, such as an additional carbon footprint and embodied energy, which is related to inadequate runway performance [8]. Although the coronavirus 2019 (COVID-19) global pandemic caused an unprecedented decline on seats offered worldwide by commercial airlines of approximately 60% in 2020 [9], a shift in the aviation industry is expected to occur towards adopting greener and more efficient travelling methods [10]. Following a few years of recuperation, the aviation industry is anticipated to make a full recovery [11]. Airports will likely once again be operating at pre-pandemic levels in terms of demand and may even become busier. As an example, Santiago's main airport in Chile, Arturo Merino Benítez International Airport (ICAO: SCL), is one of the busiest in Latin America: at its peak before COVID-19, the airport managed either a take-off or departure operation on its primary runway on average every 3 minutes. Nowadays, and perhaps more than ever, safe, rapid, and efficient procedures are needed to measure airfields pavements' condition and roughness.

The Chilean airport system comprises airfields grouped into three layers of importance: (i) the primary network, which comprises 16 airports essentially aimed at managing international flights, (ii) the secondary network, which comprises airports mainly intended for managing domestic flights, (iii) the aerodromes network, which comprises the small airports located in rural, secluded areas that service small communities by connecting them with urban zones. The entire system comprises 300+ airports and aerodromes, of which approximately one third is part of public infrastructure. This work is based on the study of three airports within the primary network.

For airport pavement condition assessment, the Pavement Condition Index (PCI) is a parameter that is widely used in airfield pavement management. Extensive research has been conducted involving the use of the PCI, for which there appears to be an agreement regarding its suitability and appropriateness as it concerns airport pavement engineering. Conversely, pavement roughness assessment is a more contentious issue: this is because there appears to be a large number of parameters that have been used for airfields, both at the research and industry levels. A parameter that has attracted considerable interest is the International Roughness Index (IRI), which was developed for highway pavement surfaces. As such, it is theoretically not applicable to airport pavements. Nevertheless, as a parameter that is extremely familiar to pavement engineers, IRI has indeed been used extensively to assess the roughness of airport pavements. Therefore, its validity in the context of airfields is continually worth exploring and discussing, as is studying its potential relationship with pavement conditions.

This article is based on the assessment of three runways at mid-size Chilean airports and aims to establish the prospective relationship that may exist between the two parameters that are traditionally used to measure pavement roughness and condition, i.e. the IRI and PCI, respectively, which were measured using semi-automated processes. In addition, an automated methodology is proposed that is parsimonious in nature to estimate both the IRI and PCI, based on a digital image processing algorithm that accurately determines the total amount of cracking in the pavement, and which requires essentially no human intervention. This article is organised as follows: Section 2 provides an updated literature review on the subject to establish the current state-of-the-art knowledge on airport pavement roughness and condition assessment as well as attempts to correlate both properties and recent trends in the field; Section 3 explains in detail the research process carried out in this work; Section 4 establishes the methodology of data acquisition and processing methodology, which served as the foundation for developing the roughness and condition predictive models described in Section 5. Finally, the conclusions of this work are summarised in Section 6.

2 Literature Review

The role of an airport pavement management system (APMS) is to provide support to the technical, engineering, and management activities of airport personnel who are responsible for providing a pavement infrastructure that is safe and efficient for aircraft operation [12]. It is widely accepted that an APMS comprises six basic components, as shown in Figure 1 [1, 13].

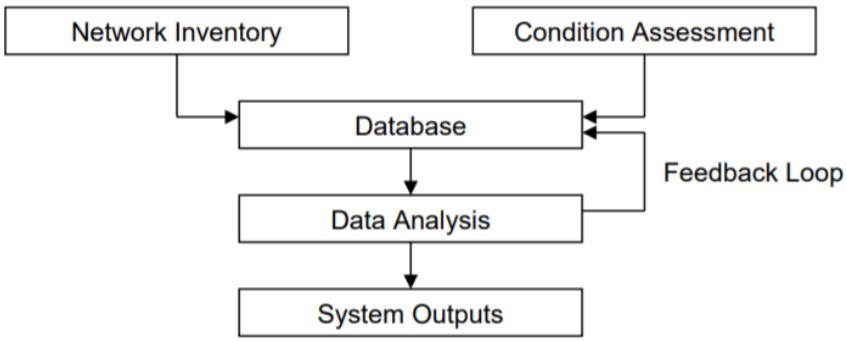

Figure 1. The basic components of an airport pavement management system [1]

'Network inventory' defines the physical characteristics of the set of pavements being managed, e.g. pavement geometrics and sections, drainage, construction details, traffic, and maintenance programmes [14]. A network inventory serves as the foundation of an APMS. 'Condition assessment' involves the evaluation of pavement surface distress, roughness, friction, the presence of foreign debris, and the evaluation of pavement surface deflections [12]. In an APMS, the PCI is used for an operational surface to establish both the condition and the structural integrity of the pavement. The PCI is obtained following the procedure described in ASTM D5340-20, Standard Test Method for Airport Pavement Condition Index Surveys [15] and is calculated by performing a pavement survey that aims to register and analyse its distress types, severity, and quantity by assigning a score from 0 to 100, with 100 reflecting a pavement in excellent condition. Extensive research has been published on airport pavements regarding the use of PCI for estimating their condition ([4], [16], [3], [17]), for which there appears to be an agreement within the technical community regarding the appropriateness of this parameter's use. Conversely, for pavement roughness assessment, a more divergent approach can be found in the literature concerning its use for airports; see, e.g. Loprencipe and Zoccali [18] and Woods and Papagiannakis [19] for comprehensive

discussions on this issue. One parameter that seems to attract substantial research interest is the IRI, which was originally proposed in 1986 by two World Bank documents ([20], [21]) and formally standardised in ASTM E1926-08 (Reapproved 2021): Standard Practice for Computing International Roughness Index of Roads from Longitudinal Profile Measurements [22]. The IRI is calculated using a mathematical approach based on a quarter-car model, where its accumulated distance travelled upwards and downwards as it moves in a longitudinal profile is a measure of the surface roughness, as shown in Equation 1 as follows:

$$IRI = \frac{1}{l}\int_0^{l/v} |\dot{z}_s - \dot{z}_u| \, dt \tag{1}$$

where l is the profile length in km, ν is a simulated speed of 80 km/h, $\dot{z}_s$ is the time derivative of the vertical displacement of the sprung mass, and $\dot{z}_u$ is the time derivative of the vertical displacement of the unsprung mass. Although IRI is not specifically designed for airport pavements, there is an extensive body of technical literature that addresses the use of IRI for the roughness assessment of airfield pavements (e.g. [23], [24], [25], [3], [26], [27], [28], [29], [30]), among which several are intended for specific use in airports located in Brazil, Italy, Mexico, South Africa and Canada. Although some international regulations (e.g. ICAO [31]) do not include the IRI as a parameter for the roughness evaluation of airport pavements (and some authors have even discouraged its use for airfields [32]), its extensive use and experience for highway pavements make the IRI an attractive choice for practitioners and researchers on the subject. Several other parameters have also been used for pavement roughness assessments at airfields including those noted below:

- The Boeing Bump Index (BBI) was developed for what is considered the most critical condition of runway roughness, i.e. a heavily loaded aircraft approaching take-off speed [33]. The BBI is currently included in America's Federal Aviation Administration's (FAA) regulations [34] and is largely regarded as an acceptable and adequate parameter for the roughness evaluation of airport pavements [18], [35].

- The Runway Roughness Index (RRI) was proposed by the FAA, based on human factors, and is defined in terms of the weighted root-mean-square of acceleration at the pilot station [36].
- The Ride Comfort Index (RCI) is a subjective method of rating the roughness of a pavement using a scale of 0 to 10, with 10 representing a very good ride quality; however, it is acknowledged that this index is not appropriate for indicating the presence of individual bumps of excessive magnitude [30].
- The Root Mean Square Vertical Acceleration (RMSVA) is calculated for 100-metre sections to identify any portions of the runway profile that have higher roughness levels as part of the entire runway profile [30], [35].
- The Landing Gear Cumulative Stroke (LGCS) refers to the dynamics associated with the nose landing gear, which combines the advantages of both the BBI and IRI [37], [38].
- The Main Landing Gear Cumulative Stroke (MLGCS) is a recently developed index, that makes use of the cumulative stroke of the main landing gear instead of that of the LGCS to evaluate roughness; it has been found to provide a better correlation in comparison to both BBI and IRI [39], [38].
- The Full Aircraft Roughness Index (FARI), based on the modelling of an aircraft by using three degrees of freedom (pitching angle, transverse roll angle and vertical displacement) simultaneously has shown a better correlation than the IRI and RMSVA with runway roughness estimation [40].

There have been extensive research efforts reported in pavement engineering literature that established empirical relationships between roughness and distress, although intended for highway pavements. For example, Kirbas [41] studied the effect that some typical pavement distresses have on the IRI. An overall coefficient of determination of $R^2 = 0.745$ was obtained in this regression model that estimates the IRI depending on distress types such as alligator cracking, bleeding, block cracking, corrugation, among others. In addition, Lin et al. [42] analysed correlations between the repair of some typical types of distress and the associated improvement in the IRI. These correlation analyses were performed using artificial neural networks obtaining varying coefficients of determination from $R^2 = 0.537$ to 0.945. Such

results are in agreement with the study published by Sandra and Sarkar [43], who obtained a coefficient of determination of $R^2 = 0.986$ for a predictive model for the IRI depending on distress types such as ravelling, patching, potholes, cracking, and rutting. Some other studies have been published that address empirical relationships between roughness and condition, although adding other external variables in the analysis. For example, Abd El-Hakim and El-Badawy [44] reported a predictive model for the IRI using artificial neural networks, in which neurons in the input layer included the pavement age, a freezing index as well as distress types, such as cracking, spalling, and patching. This model achieved a coefficient of determination of $R^2 = 0.828$ (a more modest value of $R^2 = 0.584$ was obtained when using a more traditional approach based on regression analysis). In this line, other studies, such as those published by Gong et al. [45] and Janani et al. [46], developed predictive models for the IRI based on pavement distress measurements, but including other aspects such as traffic, climate conditions, maintenance, and structural data. These studies also concluded that distress types are strongly correlated to the IRI. Finally, there have also been research attempts to explicitly correlate the roughness and condition parameters of interest in this work, namely the IRI and PCI, respectively. For example, Park et al. [47] proposed a linear model between the logarithm of both the PCI and IRI and found a maximum coefficient of determination of $R^2 = 0.66$. Another related work has been recently reported by Adeli et al. [48] who proposed a piecewise linear model for the PCI depending on the IRI, reporting varying coefficients of determination from $R^2 = 0.59$ to 0.76. In addition, Ali et al. [49] reported a linear model to predict the PCI depending on the IRI, having a coefficient of determination of $R^2 = 0.79$. It is worth remembering that all articles mentioned in this discussion were intended for road pavements; therefore, there is currently a gap in the literature where applications of this field in airport pavements need to be studied. Regarding technologies for use in pavement asset management, Peraka and Biligiri [14] have reported the most recent review at the time of writing. Such review highlighted the advent of new trends based on image processing and artificial intelligence techniques, which is in line with the methodology proposed in this work for estimating the PCI and IRI.

3 Research Methodology

This work was carried out following the four stages summarised in Figure 2. In stage 1, three medium-size airfields were selected within the Chilean airport system. The airfields selected were the following: (i) La Florida Airport, located in the city of La Serena (ICAO: SCSE), (ii) Chacalluta Airport, located in the city of Arica (ICAO: SCAR), and (iii) El Loa Airport, located in the city of Calama (ICAO: SCCF). Figure 3 shows aerial photographs of the three airports studied in this work, and Table 1 presents a summary of their location and runway characteristics. This work only considered analyses carried out on the runways of the airports shown in Figure 3.

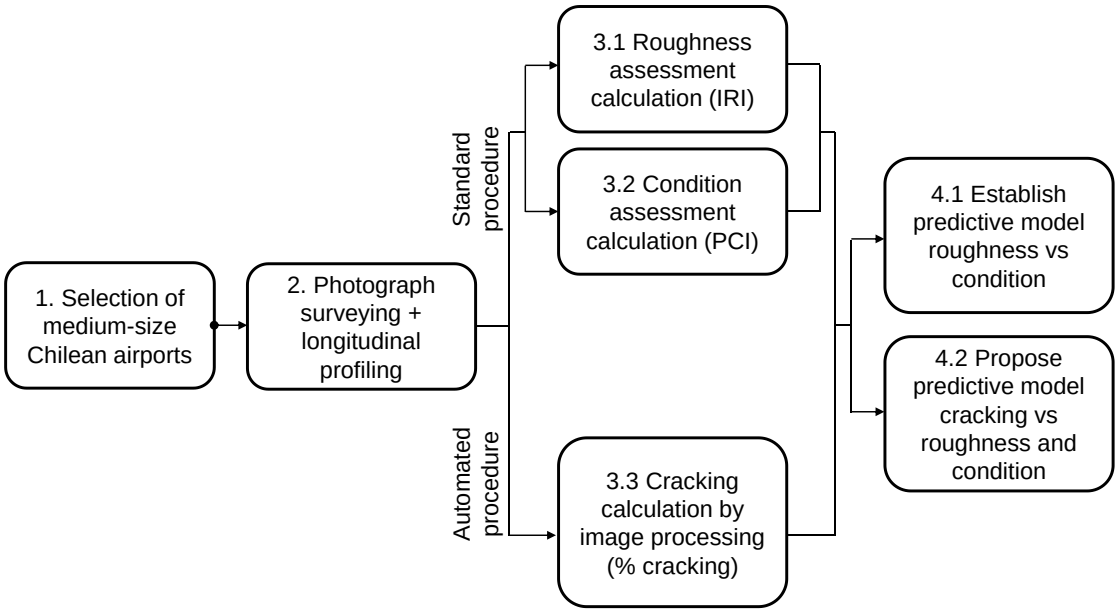

Figure 2. The research methodology that was followed in this work

Table 1. A summary of the characteristics of the three airports studied in this work

	Airport		
Description	La Florida	Chacalluta	El Loa
City	La Serena	Arica	Calama
Latitude	29º 54' 59" S	18° 20' 55" S	22° 29' ′23" S
Longitude	71º 11' 58" W	70° 20' 19" O	68° 54' ′13" O
Elevation (masl)	147	49	2,326
Runway length (m)	1,938	2,170	3,040
Runway width (m)	45	45	45
Material	Asphalt	Asphalt	Asphalt

(a)

(b)

(c)

Figure 3. Aerial photographs of the three airfields studied in this work: (a) La Florida Airport, (ii) Chacalluta Airport, and (iii) El Loa Airport.

In stage 2, a comprehensive photograph survey was carried out to capture the entire length and width of the three runways shown in Figure 3 by using an experimental setup that is detailed in Section 4.1. Examples of these photographs are shown in Section 4.1, where their ability to capture a wide range of pavement distress types can be observed. In addition, longitudinal profiling was performed on the three runways in order to estimate the pavement

roughness. These data allowed the study to move on to stage 3, which comprised two approaches as follows: (i) a standard procedure aimed at making calculations for the pavement condition using the PCI and pavement roughness using the IRI, and (ii) an automated procedure that aimed to determine the cracking percentage by using a MATLAB-based algorithm in image analysis. Once both approaches were completed, stage 4 followed, which involved conducting regression analyses for establishing the correlation that may have been present between the IRI and PCI, as well as proposing predictive models that incorporated the total cracking percentage in a sampling unit as a parameter for correlation with the PCI and IRI.

4 Data Generation and Processing

4.1 The IRI and PCI Calculations – Standard Procedure

In this study, both IRI and PCI field measurements were carried out using a Laser Crack Measurement System (LCMS) that has been attached at the back of a van-type vehicle (an image of the actual equipment setup is available online [50]). The LCMS used in this work is a 3D scanning system able to automatically detect roughness and some types of distress (therefore some others need to be surveyed manually). The technical specifications of this system are described as follows:

- Number of laser profilers: 2
- Height of the profilers: 2.5 m at 90° relative to the pavement
- Transversal field of view: 4.0 m
- Vehicle speed: up to 100 km/h
- Transverse resolution: 1 mm
- Depth resolution: 0.5 mm
- Sampling rate: 200 profiles/s
- Profile spacing: 15 cm

In this study, the PCI calculations for the runways were carried out using a semi-automated process comprising the following steps: (i) the definition of branches and sections of the included airfields; (ii) the definition of sampling units in terms of size and location for all of

the sections defined; (iii) photographic surveying of the airfields in their entirety; (iv) a fitting and matching procedure of images to sections; (v) the classification of distresses and PCI calculations (performed using a mixed procedure that has an automatic part to determine volumetric distresses, and a manual part to determine superficial distresses), following ASTM D5340-20 [15]. This procedure allowed for calculating the PCI for 100% of the sampling units associated with each of the analysed runways. For example, taking the case of Chacalluta Airport, Figure 4b shows the branches and sections defined for the airfield, where four branches and 19 sections are selected. The four branches were defined using the following code: PIs are related to the runway, Us are associated with the thresholds, RAs, DBs and DCs are related to the taxiways, and PLs are associated with apron platforms. For the current study, only PIs were selected for analysis. For the example of Chacalluta Airport the number of sampling units were as follows: PI-1 comprised 19, PI-2 comprised 82, PI-3 included 54 and PI-4 had 8, totalling 163 sampling units for this airport. The area of each sampling unit was approximately 450 m^2, with a 4-metre width and a varying length to cover the entire length of the corresponding section. Figure 5 shows some photographs of sampling units belonging to Chacalluta Airport's runway (the PIs in Figure 4) and their corresponding PCI value.

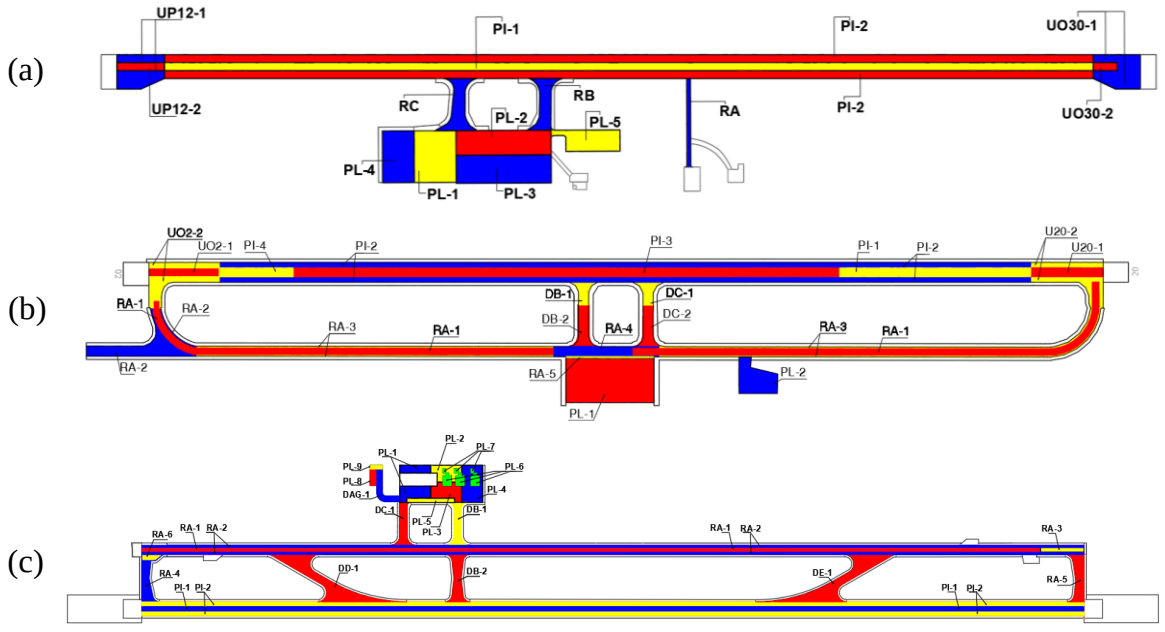

Figure 4. Branches and sections selected for the three airports studied in this work: (a) La Florida Airport, (b) Chacalluta Airport, and (c) El Loa Airport.

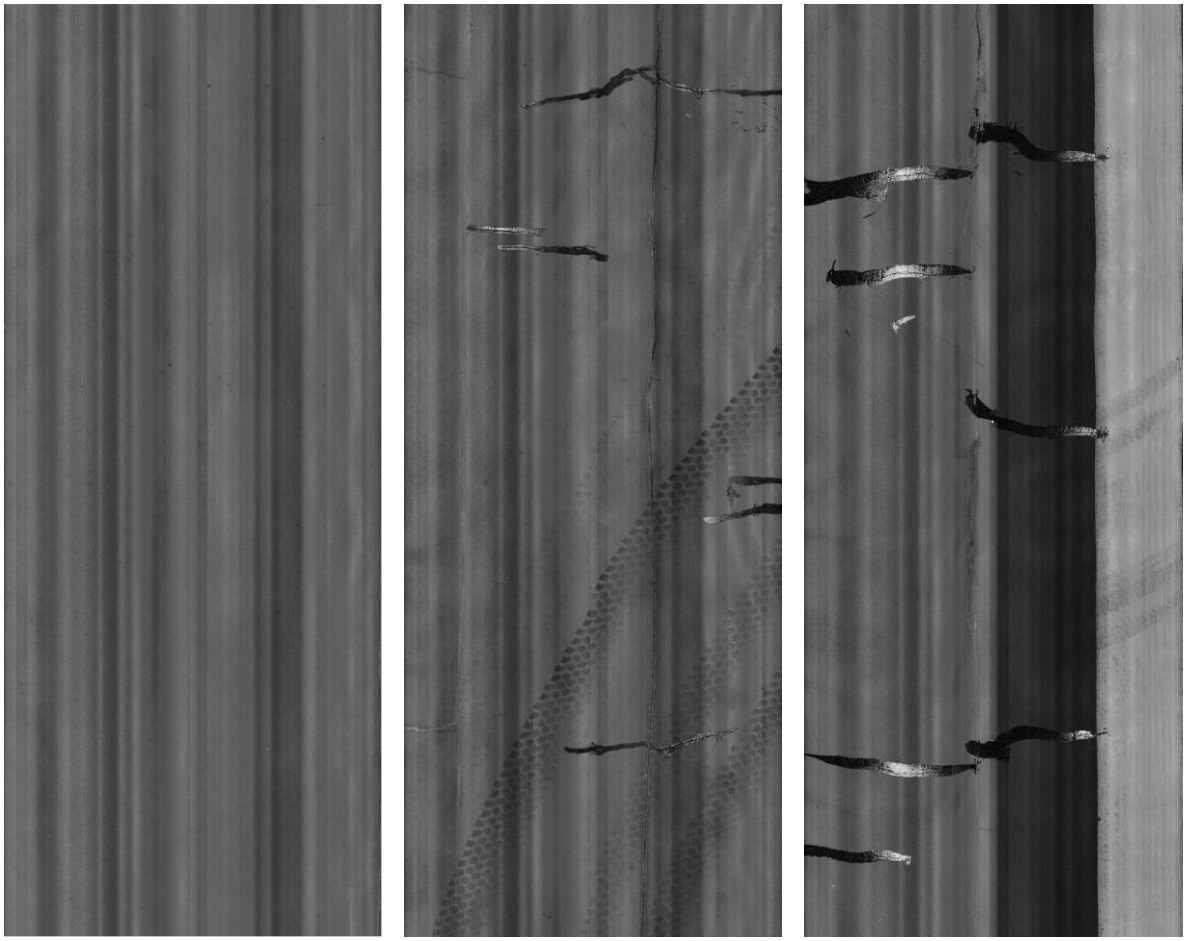

(a) (b) (c)

Figure 5. Sampling units of Chacalluta Airport's runway with varying PCI parameters. (a) PCI = 98; (b) PCI = 70; (c) PCI = 57.

The parameter IRI was calculated using an industry-standard procedure stated in ASTM E1926-08 (Reapproved 2021) [22] that was performed in several profiles along the runways. For example, for La Florida Airport, eight profiles were taken on each side of the runway centreline, at distances of 1, 3, 5, 7, 9, 11, 13, and 15 m for 100-metre-long sections. Figure 6 shows a sample of the IRI profiles for +3, +9, -3, -9 m from the runway centreline. Table 2 summarises the IRI calculations for the entire runway of the above-mentioned airport.

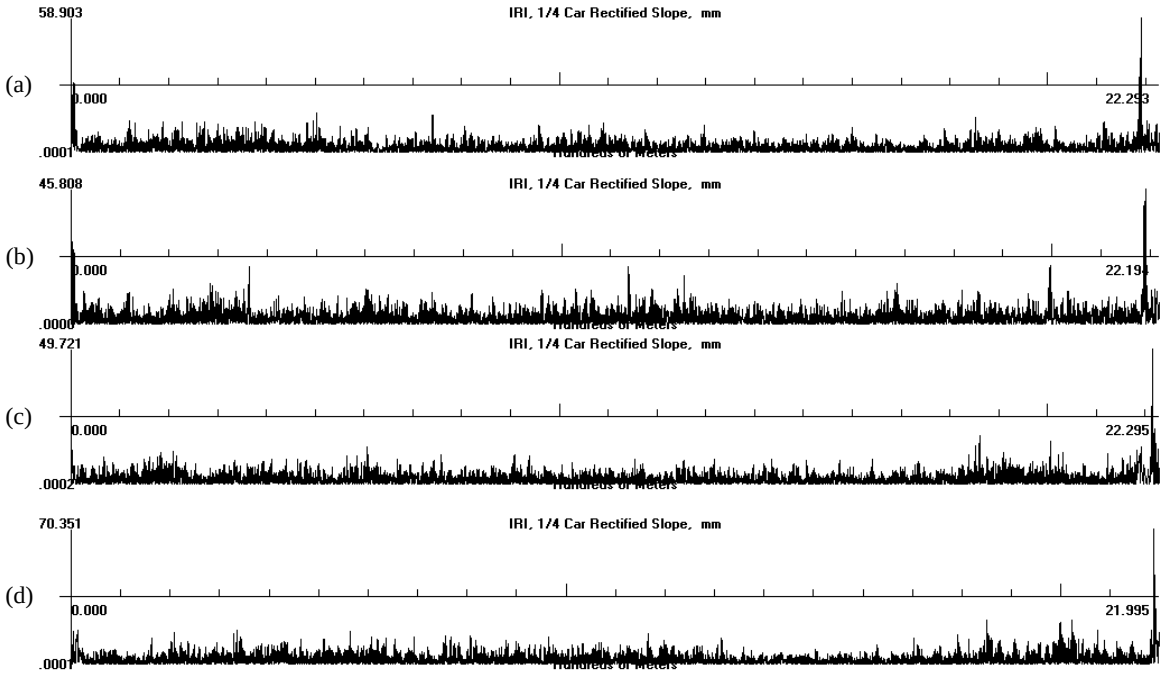

Figure 6. A sample of the IRI profiles for La Florida Airport's runway measured from the centreline at a distance of (a) +3m, (b) +9m, (c) -3m, (d) -9m.

Table 2. The IRI values for the entire runway of La Florida Airport.

		IRI (m/km)															
		Profile (distance to runway centerline)															
Section	Length (m)	+ 15 m	+ 13 m	+ 11 m	+ 9 m	+ 7 m	+ 5 m	+ 3 m	+ 1 m	- 1 m	- 3 m	- 5 m	- 7 m	- 9 m	- 11 m	- 13 m	- 15 m
1	100.0	2.656	2.270	2.669	3.157	2.802	3.163	3.645	3.316	2.856	3.585	3.556	3.048	3.195	2.582	3.412	2.728
2	100.0	2.580	2.275	3.289	2.804	3.107	2.833	2.116	2.222	2.072	2.827	3.331	2.650	4.249	2.471	2.491	2.791
3	100.0	2.869	2.478	3.273	1.950	3.304	3.036	2.167	2.712	2.833	3.415	3.439	2.302	2.553	2.290	2.694	2.894
4	100.0	2.476	1.507	2.316	2.499	3.771	3.345	2.508	2.406	2.085	3.172	3.100	2.494	2.663	2.202	3.794	2.179
5	100.0	2.704	2.252	2.331	2.185	3.374	3.198	2.162	2.818	2.236	4.389	3.880	2.870	2.895	2.963	3.959	2.497
6	100.0	2.630	2.383	3.732	2.588	2.833	2.602	2.201	2.457	2.036	3.106	3.490	2.678	2.548	2.646	3.627	2.948
7	100.0	2.548	2.034	2.925	2.220	2.668	2.279	1.925	2.989	1.859	2.874	3.059	3.077	2.704	2.526	2.402	2.494
8	100.0	2.865	2.069	3.018	2.498	2.824	2.744	2.444	2.911	1.639	2.538	2.666	2.394	2.390	1.994	2.411	3.441
9	100.0	2.876	2.015	2.467	2.203	2.085	2.068	1.889	3.060	2.333	2.428	2.260	3.586	3.115	2.978	2.943	3.149
10	100.0	3.671	2.321	2.088	2.242	3.225	3.107	1.960	3.114	1.475	2.634	2.066	2.482	3.664	2.771	2.792	3.374
11	100.0	2.188	1.611	2.679	2.524	1.635	1.933	1.550	2.927	1.451	2.315	2.344	2.324	2.489	2.244	1.950	2.334
12	100.0	2.772	1.917	2.769	2.425	2.170	2.451	1.665	2.184	2.279	2.773	1.824	2.450	2.148	1.974	2.019	2.228
13	100.0	2.386	1.614	2.157	2.241	1.805	2.002	1.846	2.519	2.309	2.733	2.158	1.540	2.842	2.457	2.421	2.425
14	100.0	2.843	2.192	3.172	2.982	2.443	2.485	1.897	2.353	2.400	3.093	3.089	2.141	3.482	3.086	2.490	2.842
15	100.0	2.325	2.009	2.888	2.134	2.498	2.464	2.283	2.357	2.641	3.389	2.458	2.560	3.444	2.754	2.563	3.468
16	100.0	2.537	1.984	3.437	1.741	2.773	2.815	2.588	3.174	2.130	4.046	2.913	2.571	2.383	2.259	2.436	3.195
17	100.0	2.575	1.950	2.102	1.682	2.372	2.599	2.725	3.120	3.221	4.434	4.142	3.443	3.667	3.254	2.952	1.897
18	100.0	2.534	2.163	2.413	1.995	2.788	2.890	2.635	2.284	2.864	4.104	4.313	2.924	3.761	2.749	3.150	2.623
19	100.0	2.825	2.441	3.258	2.641	2.910	2.848	2.402	2.661	2.671	3.213	2.948	3.334	4.639	2.694	3.738	3.392
20	54.9	4.160	4.263	4.284	3.990	5.301	5.304	5.788	4.622	3.939	4.668	5.677	4.951	5.565	4.852	5.546	4.107

4.2 Cracking Percentage Calculations – Automated Procedure

For this work, a MATLAB-based code was developed that was able to determine the cracking percentage using digital image processing techniques. The code was developed using the

Digital Image Analysis Toolbox provided by MATLAB, with some in-house extensions that were suitable for the type of analysis required in this work. Figure 7 shows a sample of the images processed using the developed code and reflects an ability to detect a wide range of cracking. It is worth noting that this process of obtaining cracking percentage requires essentially no human intervention other than loading the seed images for analysis, making the process fully automated. All of the images described in Section 4.1 that were used as aids for PCI calculations were processed using the MATLAB code developed for this work. Therefore, for each sampling unit of the runway, data are available in terms of their PCI, IRI, and total cracking percentage. These data allowed for the generation of predictive models using these parameters, as it is described in the following section.

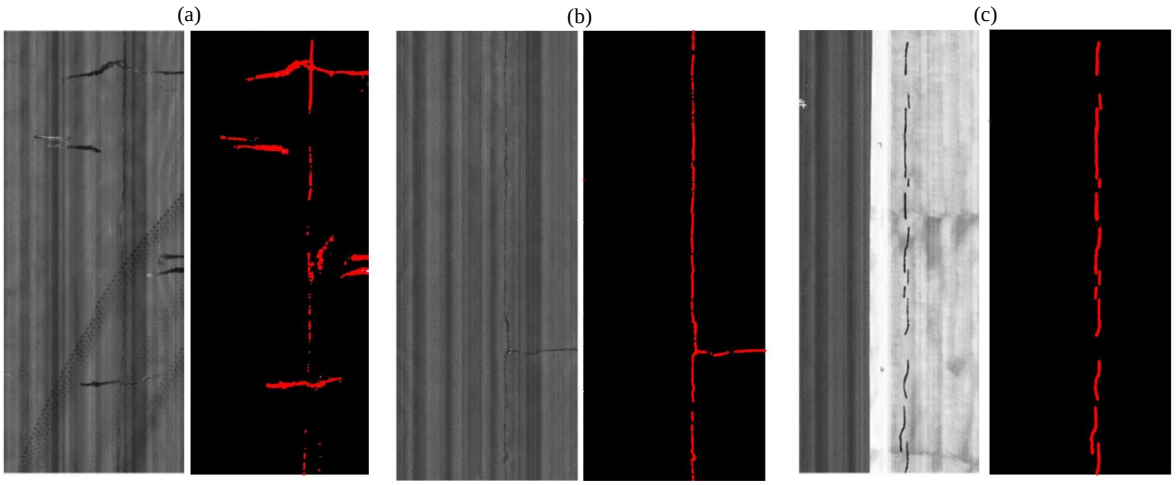

Figure 7. Three examples of image processing for cracking percentage determination: the left-hand side image is the unprocessed photograph, and the right-hand side image is the corresponding processed image.

5 Roughness and Condition Predictive Models

The information described in previous sections allowed defining for each sampling unit of the runways studied in this work their corresponding PCI, IRI and total cracking percentage, which made it possible to derive statistically meaningful correlations among these parameters. Figure 8 shows some examples of sampling units and their PCI, IRI and total cracking percentage. The predictive models were obtained using nonlinear regression analysis techniques and a dataset comprising 8,275 images and their corresponding PCI, IRI, and cracking percentage, comprising a final total of 24,825 data points. The following

sections detail the regression results for establishing a correlation between pavement roughness and condition, which were measured following traditional procedures. Additionally, the results were used to establish a correlation between the pavement cracking percentage that was measured following an automated procedure and both pavement roughness and condition.

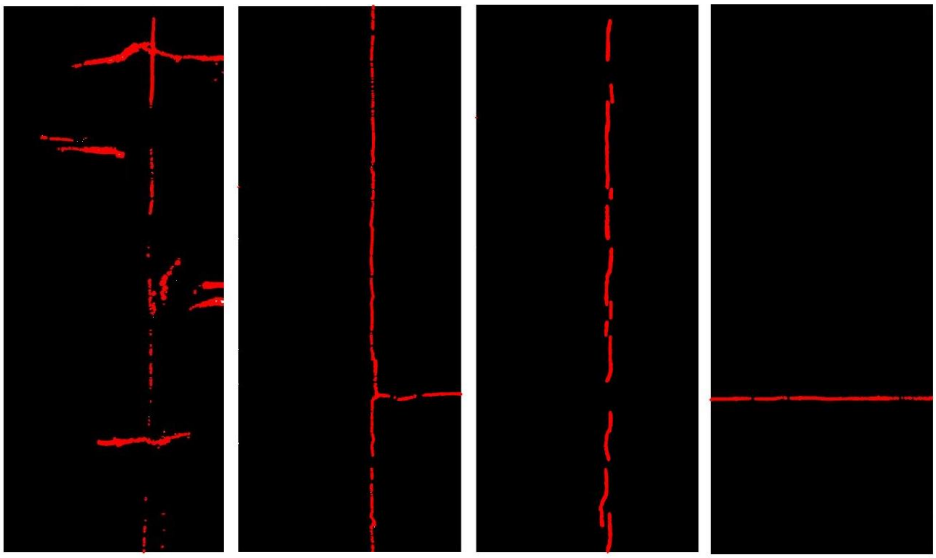

% Cracking	0.377	0.216	0.214	0.0328
PCI	70	76	74	81
IRI (m/km)	4.700	3.585	3.585	2.085

Figure 8. Sampling unit examples and their corresponding cracking percentage, PCI and IRI.

5.1 Roughness vs. Condition

The first correlation that was performed served as an attempt to establish a statistically meaningful relationship between the pavement roughness and condition using the IRI and PCI, respectively. As previously noted in Section 4, both parameters were measured by using industry-standard procedures. It is worth mentioning that when performing the analysis of all images and their corresponding IRI and PCI, it was possible to observe that some small subsets of images had assigned the same IRI value but different PCI values within a limited range. Therefore, in order to carry out the regression analysis between IRI and PCI, the average value of PCIs was used which was then associated to their single corresponding IRI

value. Figure 9 shows the data points for IRI and their corresponding average PCI, and a power fitted curve, obtained via nonlinear least-squares test using the Levenberg-Marquardt algorithm, where a coefficient of determination of $R^2 = 0.895$ was obtained. The functional form of this predictive model is shown in Equation 2 with the regression coefficients and their 95% confidence bounds shown in Table 3. The scatter plot of residuals for this regression are shown in Figure 10 where it is possible to see that the variance of the residuals does not show a tendency across the full range of the fitted values. It is noted that the predictive capacity of this model is comparable with other correlations between PCI and IRI reported in the literature, despite these having been obtained for highway pavements (see Section 2).

$$Log_{10}(PCI) = a \cdot Log_{10}(IRI)^b + c \quad (2)$$

Table 3. Regression coefficients and their 95% confidence bounds for Equation 2

a	b	c
-0.574	**3.030**	**1.986**
(-0.751; -0.398)	(2.379; 3.681)	(1.977; 1.995)

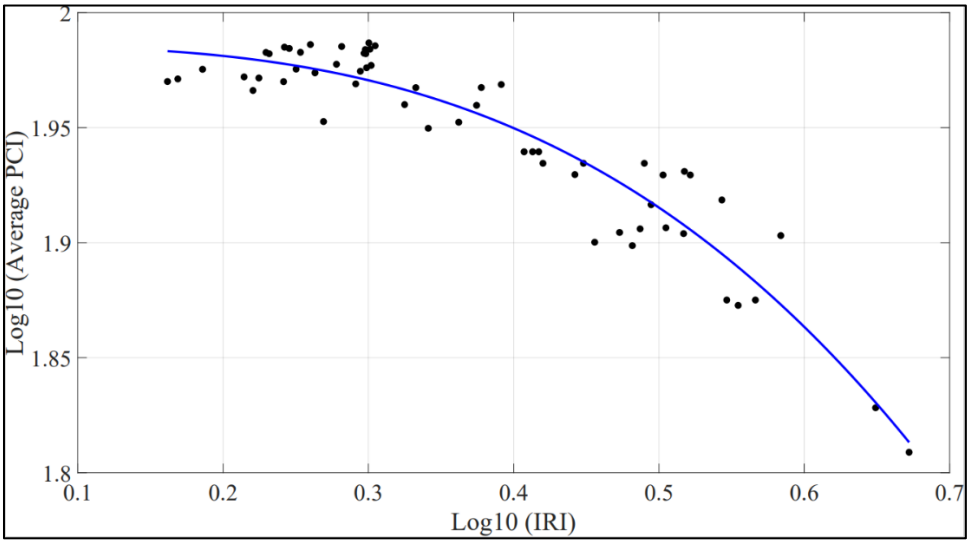

Figure 9. Data points and power fitted curve between the IRI and the average value for their corresponding PCI for all the runways included in this study.

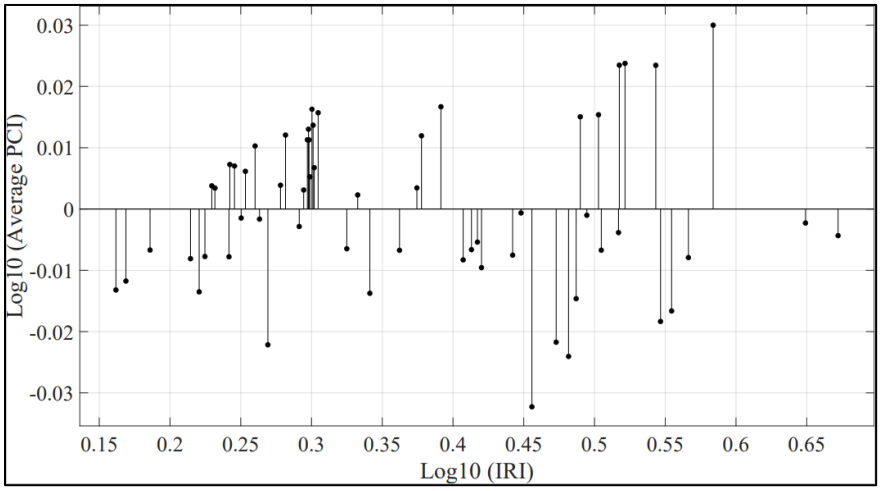

Figure 10. Scatter plot of residuals for the correlation shown in Figure 9.

The predictive model proposed in Equation 2 with the regression coefficients stated in Table 2 was compared with a previously reported predictive model IRI vs PCI, although for application in highway pavements, namely, the model reported in Park et al. [47]. Figure 11 shows a PCI comparison between values measured and predicted with the two models, using the same sample of IRI values. From this figure, it is possible to see that less scatter and lower PCI estimations (and therefore more conservative predictions) are obtained when using the model proposed in this work for airports in comparison to those reported for highways.

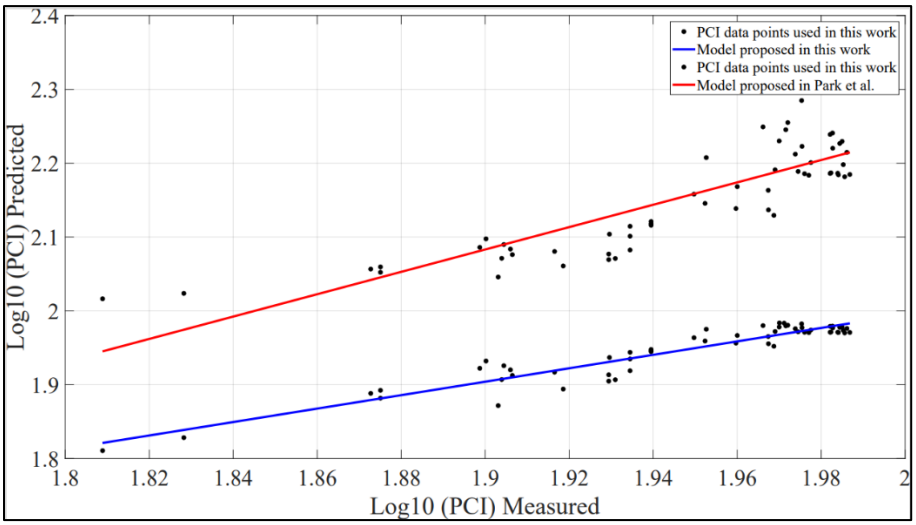

Figure 11. Comparison of PCI estimations between the predictive model proposed in this work and the predictive model for highway pavements proposed in Park et al. [47], using the same sample of IRI values.

5.2 Cracking percentage vs Roughness and Condition

This section details the potential correlations that are likely to exist between pavement roughness and condition in relation to the total cracking percentage found in a sampling unit. Initially, a predictive model for the IRI was proposed as a function of the square root of the total cracking percentage. It is worth noting that when analysing the dataset, it was possible to observe that small subsets of images had been assigned the same square root of the total cracking percentage but different IRI values within a limited range. Therefore, rather than including all data points in the regression analysis, it was decided that for each IRI value, the average for the square root of the total cracking percentage was used as their corresponding value. Figure 12 shows the data points for the average square root of the total cracking percentage and their corresponding IRI values, where a linear regression model has been proposed whose functional form is stated in Equation 3 with the regression coefficients and their 95% confidence bounds shown in Table 4. This predictive model has a coefficient of determination of $R^2 = 0.834$. The scatter plot of residuals for this regression are shown in Figure 13 where it is possible to see that the variance of the residuals does not show a tendency across the full range of the fitted values.

$$IRI\ (m/km) = c \cdot \sqrt{(\%\ cracking)} + d \tag{3}$$

Table 4. Regression coefficients and their 95% confidence bounds for Equation 3

c	d
4.340	**1.819**
(3.827; 4.854)	(1.708; 1.930)

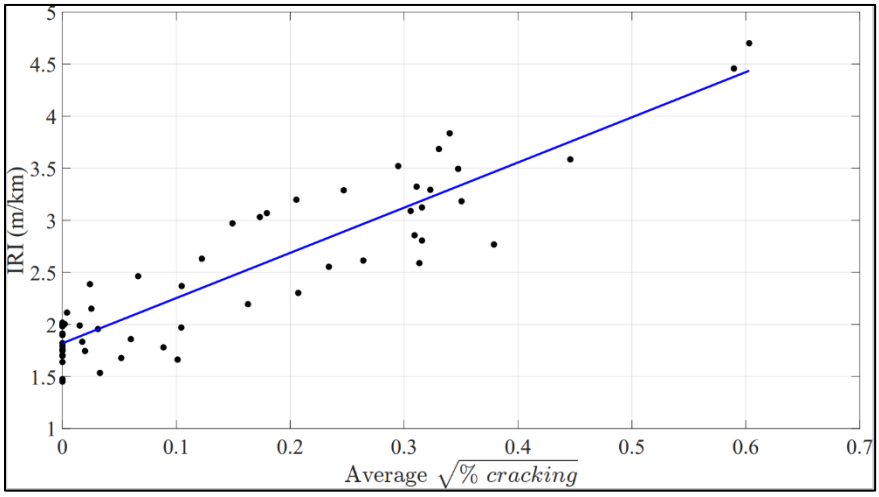

Figure 12. The data points and the linear regression model between the square root of the total cracking percentage (on average) and the IRI (m/km).

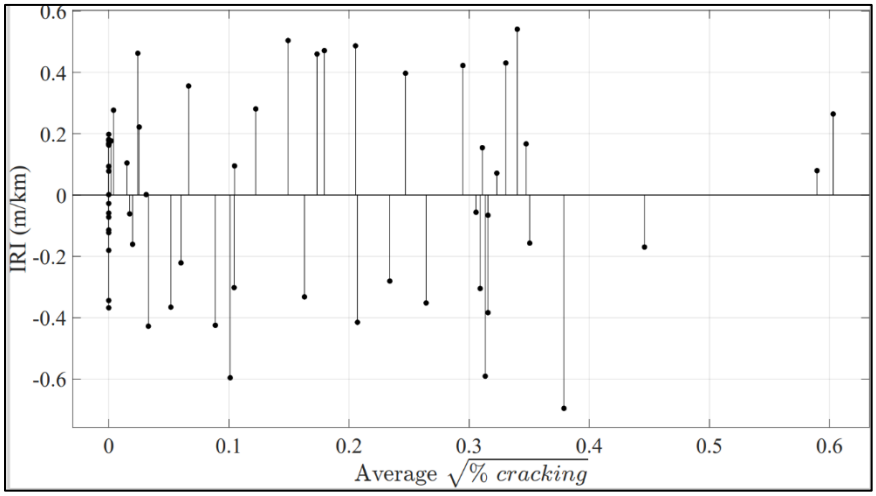

Figure 13. Scatter plot of residuals for the correlation shown in Figure 12.

Finally, a predictive model for the PCI as a function of the cracking percentage is proposed. In a similar manner to the predictive model described in Figure 12, it is worth noting that when analysing the dataset, it was possible to observe that small subsets of images had been assigned the same square root of the total cracking percentage but different PCI values within a limited range. Therefore, rather than including all data points in the regression analysis, it was decided that for each PCI value, the average for the square root of the total cracking percentage was used as their corresponding value. Figure 14 shows the data points for the average square root of the total cracking percentage and their corresponding Log_{10}(PCI)

values, where a linear regression model has been proposed whose functional form is stated in Equation 4 with the regression coefficients and their 95% confidence bounds shown in Table 5. This predictive model has a coefficient of determination of $R^2 = 0.842$. The scatter plot of residuals for this regression are shown in Figure 15 where it is possible to see that the variance of the residuals does not show a tendency across the full range of the fitted values.

$$Log_{10}(PCI) = e \cdot \sqrt{(\%\ cracking)} + f \tag{4}$$

Table 5. Regression coefficients and their 95% confidence bounds for Equation 4

e	f
-0.262	**1.979**
(-0.306; -0.218)	(1.965; 1.992)

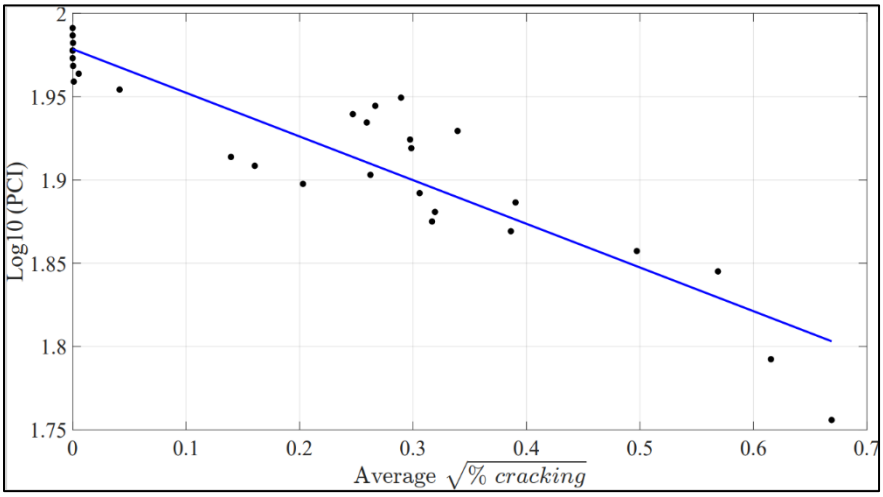

Figure 14. The datapoints and the linear regression model between PCI and $\sqrt{(\%\ cracking)}$

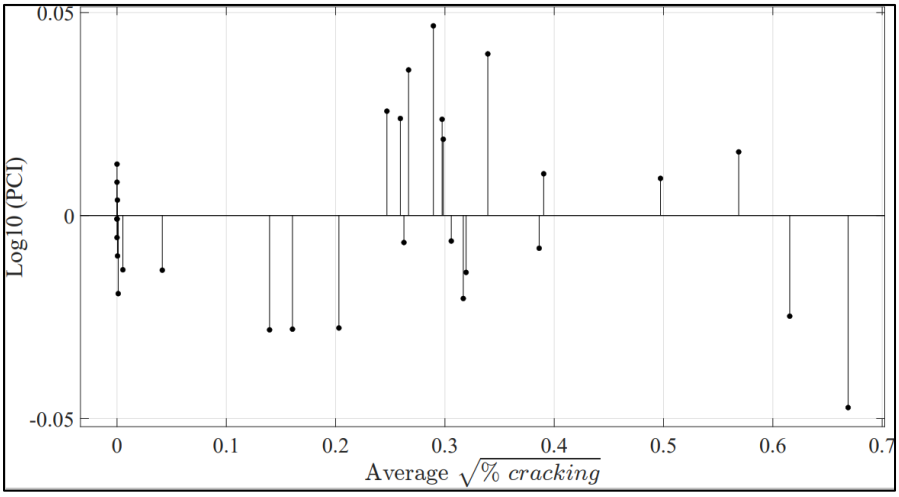

Figure 15. Scatter plot of residuals for the correlation shown in Figure 14.

6 Conclusions and further research

Airport pavement roughness and condition correlations were proposed based on the analysis of 8,275 images of three runways of mid-size airports in Chile. This work used industry-standard methodologies to assess two parameters that are traditionally used to measure roughness and condition, i.e. IRI and PCI. Although the IRI parameter has not been devised for use in airport pavements, its extensive use at both the research and industry levels makes it relevant for investigation in this work. The study results suggest that there is a statistically reasonable level of correlation between IRI and PCI (predictive capacity, $R^2 = 0.895$) and, as such, it can be used to provide useful information for airport management agencies to ensure timely maintenance decisions. In addition, an automated, parsimonious, and virtually inexpensive method for estimating both the IRI and PCI was proposed, based on an automated image analysis procedure that required no human intervention. The image analysis procedure calculated the total amount of cracking observed in a pavement sampling unit with high accuracy. The results suggested the presence of a statistically reasonable predictive capacity for predicting the IRI ($R^2 = 0.834$) and the PCI ($R^2 = 0.842$). It is anticipated that the predictive models proposed in this work could help airport management agencies when conducting pavement condition evaluation in the context of their APMS. The simplicity of the functional forms of all the models proposed in this work (i.e. linear) is acknowledged. Further research should be carried out in trying to improve the predictive capacity of the regressions performed herein, e.g. using artificial intelligence techniques such as artificial

neural networks. In addition, it must be explored how the predictive capacity of the models proposed in this work may change for different sampling unit sizes, and accordingly, for the processing of different image sizes.

Acknowledgements

The authors extend their appreciation to the consulting company Ferrer & Asociados Ingenieros Consultores S.A. for providing information related to the IRI and PCI industry-standard calculations for all the airports studied in this article, thereby making the research possible. We also thank one of the journal's Associate Editors and an anonymous reviewer for their valuable comments that substantially improved the quality of the manuscript.

References

[1] Washington State Department Of Transportation Aviation Division, "Washington Airport Pavement Management Manual," Washington State Department of Transportation and Federal Aviation Administration, Washington, 2019. https://wsdot.wa.gov/travel/aviation/airport-management/pavement-management (Accessed: April 2022)

[2] M. Gendreau and P. Soriano, "Airport pavement management systems: an appraisal of existing methodologies," Transportation Research Part A: Policy and Practice, vol. 32, no. 3, pp. 197-214, 1998, doi: https://doi.org/10.1016/S0965-8564(97)00008-6

[3] P. Di Mascio and L. Moretti, "Implementation of a pavement management system for maintenance and rehabilitation of airport surfaces," Case Studies in Construction Materials, vol. 11, p. e00251, pp. 1-7, 2019, doi: https://doi.org/10.1016/j.cscm.2019.e00251

[4] A. F. C. Carvalho and L. G. d. Picado Santos, "Maintenance of airport pavements: the use of visual inspection and IRI in the definition of degradation trends," International Journal of Pavement Engineering, vol. 20, no. 4, pp. 425-431, 2019/04/03 2019, doi: 10.1080/10298436.2017.1309189

[5] L. Moretti, G. Cantisani, P. Di Mascio, S. Nichele, and S. Caro, "A runway veer-off risk assessment based on frequency model. Part I: Probability analysis," in Transport Infrastructure and Systems, 1st Edition ed. London: CRC Press, 2017, ISBN: 9781315281896

[6] L. Moretti, P. Di Mascio, S. Nichele, and O. Cokorilo, "Runway veer-off accidents: Quantitative risk assessment and risk reduction measures," Safety Science, vol. 104, pp. 157-163, 2018/04/01/ 2018, doi: https://doi.org/10.1016/j.ssci.2018.01.010

[7] D. K. McNerney and R. Harrison, "Full-cost approach to airport pavement management," Washington D.C., 1995

[8] P. Babashamsi, N. I. Md Yusoff, H. Ceylan, N. G. Md Nor, and H. Salarzadeh Jenatabadi, "Sustainable Development Factors in Pavement Life-Cycle:

Highway/Airport Review," Sustainability, vol. 8, no. 3, 248, pp. 1-21, 2016, doi: 10.3390/su8030248

[9] International Civil Aviation Organization, "Effects of Novel Coronavirus (COVID-19) on Civil Aviation: Economic Impact Analysis", Montreal, Canada, 2021, https://www.icao.int/sustainability/Documents/Covid-19/ICAO_coronavirus_Econ_Impact.pdf (Accessed: April 2022)

[10] J. Bouwer, S. Saxon, and N. Wittkamp, "Back to the future? Airline sector poised for change post-COVID-19," https://www.mckinsey.com/industries/travel-logistics-and-infrastructure/our-insights/back-to-the-future-airline-sector-poised-for-change-post-covid-19: McKinsey & Company, 2021 (Accessed: April 2022)

[11] Airports Council International, "The impact of COVID-19 on the airport business and the path to recovery," ed. https://aci.aero/news/2021/07/14/the-impact-of-covid-19-on-the-airport-business-and-the-path-to-recovery-2/: Airports Council International, 2021 (Accessed: April 2022)

[12] J. Hajek, J. Hall, and D. Hein, "Common Airport Pavement Maintenance Practices: A Synthesis of Airport Practice," Transportation Research Board - Airport Cooperative Research Program, Washington D.C., 2011, https://nap.nationalacademies.org/catalog/14500/common-airport-pavement-maintenance-practices (Accessed: April 2022)

[13] D. Lima, B. Santos, and P. G. Almeida, "Proposal of an airport pavement maintenance management system for Cape Verde," STARTCON19 – International Doctorate Students Conference + Lab Workshops in Civil Engineering, KnE Engineering, Covilhã, pp. 49-60, 2020, doi: https://doi.org/10.18502/keg.v5i5.6917

[14] N. S. P. Peraka and K. P. Biligiri, "Pavement asset management systems and technologies: A review," Automation in Construction, vol. 119, p. 103336, pp. 1-17, 2020, doi: https://doi.org/10.1016/j.autcon.2020.103336.

[15] ASTM D5340-20: Standard Test Method for Airport Pavement Condition Index Surveys, ASTM, West Conshohocken, PA, USA., 2020, https://www.astm.org/d5340-20.html (Accessed: April 2022)

[16] B. Santos, P. G. Almeida, I. Feitosa, and D. Lima, "Validation of an indirect data collection method to assess airport pavement condition," Case Studies in Construction Materials, vol. 13, p. e00419, pp. 1-8, 2020, doi: https://doi.org/10.1016/j.cscm.2020.e00419.

[17] V. Vyas, A. P. Singh, and A. Srivastava, "Entropy-based fuzzy SWOT decision-making for condition assessment of airfield pavements," International Journal of Pavement Engineering, vol. 22, no. 10, pp. 1226-1237, 2021, doi: 10.1080/10298436.2019.1671590.

[18] G. Loprencipe and P. Zoccali, "Comparison of methods for evaluating airport pavement roughness," International Journal of Pavement Engineering, vol. 20, no. 7, pp. 782-791, 2019, doi: 10.1080/10298436.2017.1345554.

[19] J. Woods and A. T. Papagiannakis, "Suitability of Runway Pavement Roughness Indices in Capturing Aircraft Response," Transportation Research Board 88th Annual Meeting, Washington D.C., USA, pp. 1-20, 2009, https://trid.trb.org/view/880729 (Accessed: April 2022)

[20] M. Sayers, T. Gillespie, and C. Queiroz, "WTP-45: The International Road Roughness Experiment. Establishing Correlation and a Calibration Standard for Measurements," The World Bank, 1986,

https://documents1.worldbank.org/curated/en/326081468740204115/pdf/multi-page.pdf (Accessed: April 2022)
[21] M. Sayers, T. Gillespie, and W. Patterson, "WTP-46: Guidelines for Conducting and Calibrating Road Roughness Measurements," The World Bank, Washington D.C., USA, 1986, https://documents1.worldbank.org/curated/en/851131468160775725/pdf/multi-page.pdf (Accessed: April 2022)
[22] ASTM E1926-08 (Reapproved 2021): Standard Practice for Computing International Roughness Index of Roads from Longitudinal Profile Measurements, ASTM, 2021, https://www.astm.org/standards/e1926 (Accessed: April 2022)
[23] J. B. Cossío Durán and J. L. Fernandes Júnior, "Airport pavement roughness evaluation based on cockpit and center of gravity vertical accelerations," Transportes, vol. 28, no. 1, pp. 147-159, 2020, doi: https://doi.org/10.14295/transportes.v28i1.1932
[24] Y. Tian, S. Liu, L. Liu, and P. Xiang, "Optimization of International Roughness Index Model Parameters for Sustainable Runway," Sustainability, vol. 13, no. 4, 2184, pp. 1-13, 2021, doi: 10.3390/su13042184.
[25] M. De Luca, "Evaluation of Runway Bearing Capacity using International Roughness Index," Transportation Research Procedia, vol. 45, pp. 119-126, 2020, doi: https://doi.org/10.1016/j.trpro.2020.02.096.
[26] Agência Nacional de Aviação Civil , "Aerodromes – operation, maintenance and emergency response" (in Portuguese), 2019, https://www.anac.gov.br/assuntos/legislacao/legislacao-1/rbha-e-rbac/rbac/rbac-153 (Accessed: April 2022)
[27] Ente Nazionale per l'Aviazione Civile, "Airport Pavement Management System - Guidelines on the implementation of a pavement maintenance management system LG 2015/003-APT – Ed. n.1 del 1 Ottobre 2015" (in Italian), 2015, https://www.enac.gov.it/repository/ContentManagement/information/P582336791/LG_2015_3_151002.pdf (Accessed: April 2022)
[28] B. González and M. Rodríguez, "Strategies to optimize the maintenance of different types of pavements used in airports in Mexico (in Spanish)," Thesis for Aeronautical Engineering degree, Instituto Politécnico Nacional, Mexico D.F., 2007, https://tesis.ipn.mx/bitstream/handle/123456789/11907/1439%202007.pdf?sequence=1&isAllowed=y (Accessed: April 2022)
[29] S. Emery, A. Hefer, and E. Horak, "Roughness of Runways and Significance of Appropriate Specifications and Measurement", 11th Conference on Asphalt Pavements for Southern Africa, South Africa: Sun City, 2015, pp. 1-10, https://www.researchgate.net/publication/281632183_Roughness_of_Runways_and_Significance_of_Appropriate_Specifications_and_Measurement (Accessed: April 2022)
[30] Transport Canada, "Measurement and Evaluation of Runway Roughness - Advisory Circular (AC) No. 302-023", 2016, https://tc.canada.ca/en/aviation/reference-centre/advisory-circulars/advisory-circular-ac-no-302-023 (Accessed: April 2022)
[31] International Civil Aviation Organization, "Annex 14 - Aerodromes - Volume I: Aerodrome Design and Operations", Canada, 2009, https://store.icao.int/en/annex-14-aerodromes (Accessed: April 2022)

[32] T. Gerardi, "Report IPRF-01-G-002-02-4: Airfield Concrete Pavement Smoothness – A Handbook " Innovative Pavement Research Foundation, Skokie, IL, USA, 2007, http://www.iprf.org/products/IPRF%20Report%2002-4%20_Final%20Publication%2004%2006%2007.pdf (Accessed: April 2022)

[33] K. J. DeBord, "Runway roughness measurement, quantification and application – the Boeing method," Boeing Commercial Airplane Group, Seattle, USA, 1995, vol. Boeing Document No. D6-81746, https://kipdf.com/runway-roughness-measurement-quantification-and-application-the-boeing-method_5ac4d8001723dd76b292fa1b.html (Accessed: April 2022)

[34] Federal Aviation Administration. Advisory Circular AC No: 150/5380-9 "Guidelines and Procedures for Measuring Airfield Pavement Roughness", 2009, https://www.faa.gov/airports/resources/advisory_circulars/index.cfm/go/document.current/documentNumber/150_5380-9 (Accessed: April 2022)

[35] S. Liu, Y. Tian, L. Liu, P. Xiang, and Z. Zhang, "Improvement of Boeing Bump Method Considering Aircraft Vibration Superposition Effect," Applied Sciences, vol. 11, no. 5, 2147, pp. 1-16, 2021, doi: 10.3390/app11052147.

[36] D. Brill, "New Runway Roughness Index (RRI): Concepts and Validation," Asociación Latinoamericana y Caribeña de Pavimentos Aeroportuarios XVI Seminar on Airport Pavements, San José, Costa Rica, 2020, (Personal communication)

[37] S. Liu, J. Ling, J. Yuan, L. Penghui, and J. Chen, "Landing Gear Cumulative Stroke-Based Runway Roughness Evaluation", Transportation Research Board 97th Annual Meeting, Washington DC, United States, pp. 1-18, 2018, https://trid.trb.org/view/1496098 (Accessed: April 2022)

[38] S. Sivakumar and A. P. Haran, "Mathematical model and vibration analysis of aircraft with active landing gears," Journal of Vibration and Control, vol. 21, no. 2, pp. 229-245, 2015, doi: 10.1177/1077546313486908.

[39] S. Liu, J. Ling, Y. Tian, and J. Qian, "Assessment of aircraft landing gear cumulative stroke to develop a new runway roughness evaluation index," International Journal of Pavement Engineering, pp. 1-12, 2021, doi: 10.1080/10298436.2021.1910823.

[40] G. Cheng and W. Guo, "Airport Pavement Roughness Evaluation Based on Three-Degree-of-Freedom Aircraft Model," Journal of Nanjing University of Aeronautics and Astronautics, vol. 48, pp. 606-614, 2016, doi: 10.16356/j.1005-2615.2016.04.024.

[41] U. Kırbaş, "IRI Sensitivity to the Influence of Surface Distress on Flexible Pavements," Coatings, vol. 8, no. 8, 271, pp. 1-19, 2018, doi: https://doi.org/10.3390/coatings8080271.

[42] J.-D. Lin, J.-T. Yau, and L.-H. Hsiao, "Correlation Analysis Between International Roughness Index (IRI) and Pavement Distress by Neural Network," Transportation Research Board 82nd Annual Meeting, Washington D.C., USA, pp. 1-21, 2003, https://www.researchgate.net/publication/228848218_Correlation_analysis_between_international_roughness_index_IRI_and_pavement_distress_by_neural_network (Accessed: April 2022)

[43] A. K. Sandra and A. K. Sarkar, "Development of a model for estimating International Roughness Index from pavement distresses," International Journal of

Pavement Engineering, vol. 14, no. 8, pp. 715-724, 2013, doi: 10.1080/10298436.2012.703322.
[44] R. Abd El-Hakim and S. El-Badawy, "International Roughness Index Prediction for Rigid Pavements: An Artificial Neural Network Application," Advanced Materials Research, vol. 723, pp. 854-860, 2013, doi: 10.4028/www.scientific.net/AMR.723.854.
[45] H. Gong, Y. Sun, X. Shu, and B. Huang, "Use of random forests regression for predicting IRI of asphalt pavements," Construction and Building Materials, vol. 189, pp. 890-897, 2018, doi: https://doi.org/10.1016/j.conbuildmat.2018.09.017.
[46] L. Janani, V. Sunitha, and S. Mathew, "Influence of surface distresses on smartphone-based pavement roughness evaluation," International Journal of Pavement Engineering, vol. 22, no. 13, pp. 1637-1650, 2021, doi: 10.1080/10298436.2020.1714045.
[47] K. Park, E. Thomas Natacha, and K. Wayne Lee, "Applicability of the International Roughness Index as a Predictor of Asphalt Pavement Condition," Journal of Transportation Engineering, vol. 133, no. 12, pp. 706-709, 2007, doi: 10.1061/(ASCE)0733-947X(2007)133:12(706).
[48] S. Adeli, V. Najafi moghaddam Gilani, M. Kashani Novin, E. Motesharei, and R. Salehfard, "Development of a Relationship between Pavement Condition Index and International Roughness Index in Rural Road Network," Advances in Civil Engineering, vol. 2021, p. 6635820, pp. 1-9, 2021, doi: 10.1155/2021/6635820.
[49] A. Ali, K. Hossain, A. Hussein, S. Swarna, H. Dhasmana, and M. Hossain, "Towards Development of PCI and IRI Models for Road Networks in the City of St. John's," Airfield and Highway Pavements, 2019, pp. 335-342, doi: 10.1061/9780784482452.033.
[50] APSA Gestión de Infraestructura, http://www.apsa.cl/equipos/#lcms (English version available), (Accessed: March 2022)